

Blurred Palmprint Recognition Based on Relative Invariant Structure Feature

Gang Wang, Weibo Wei*, Zhenkuan Pan

College of Information Engineering, Qingdao University, Qingdao, China
hellowgw@163.com, qduw@163.com

Abstract—A blurred palmprint recognition method based on Relative Invariant Structure Feature (RISF) is proposed in this paper to improve the low recognition accuracy of blurred palmprint. Firstly, the OSV decomposition model is used to obtain stable feature from blurred images. Next, a non-overlapping sampling method based on Structure Ratio (SR) for RISF is used to further improve the effectiveness of feature. Finally, Structural Similarity Index Measurement (SSIM) is introduced to measure the similarity of palmprints and judge the palmprint category for classification. Numerical experiments show that the proposed method is effective and better than some other classical algorithms.

Keywords—Blurred palmprint recognition; Relative Invariant Structure Feature; OSV decomposition model; Structure Ratio

I. INTRODUCTION

Palmprint is one important biometric feature. Palmprint recognition can be classified into three categories according to feature description and matching, including principal line extraction, subspace learning, and texture coding. The principal line extraction method [1,2] depends on the ridge information extraction using edge detection method. Palmprint image is considered as high-dimensional data in subspace learning [3,4], and the high-dimensional data is mapped to low-dimensional space using characteristic of matrix, the method have been successfully applied to face recognition, and also achieved good results when transplanted to the palm. The texture coding method [5,6] use a filter for palmprint image filtering, then encode them according to different schemes, finally, ‘and’ or ‘XOR’ operator is used to calculate the similarity between different features. The above-mentioned three methods usually use clear palmprint image captured by contact device, however, system security is also very important for identification, as a result, non-contact palmprint image acquisition and recognition research become the mainstream due to its various merits, e.g. low-cost, easy availability, high accuracy [7,8], unfortunately, defocus status might blur palmprints which was captured using non-contact device, the obtained blur palmprint is easy to degrade the performance of the recognition system. Researchers proposed some methods to solve this problem, Yuan [9] introduces image clarity evaluation standards to obtain the clear palmprint image, but it cannot be used in large-scale palmprint database. Kang [10] used a template convolution to calculate the image focus value and set threshold value based on the focus value. Wang [11] proposed an image restoration method based on

normalized super Laplace, which achieves a good experimental result. Sang [12] proposed a blurred palmprint recognition algorithm based on two-dimensional principal component analysis, which offers an effective way for further research on blurred palmprint recognition. Lin [3] state that stable features exist during the process from clear image to blurred images, and they extracted stable features by using Laplacian Smoothing Transform (LST), and achieved good recognition results when selecting the N low-frequency elements as feature vectors to recognize, but they did not explain how to select stable features.

In order to effectively extract the stable features in palmprint blurred process, a blurred palmprint recognition method based on Relative Invariant Structure Feature (RISF) was proposed. Finally, numerical experiments show that the proposed algorithm is effective and better.

II. RELATED WORKS

A. OSV Decomposition Model

In 2003, Osher et al described the texture and noise ν in $H^1(\Omega)$ spatial domain and proposed OSV image decomposition model, which can be expressed as

$$\min_{\mathbf{u}} \{E(\mathbf{u}) = \int_{\Omega} |\nabla \mathbf{u}| dx dy + \frac{1}{2\lambda} \int_{\Omega} |\nabla(\Delta^{-1}(\mathbf{f}-\mathbf{u}))|^2 dx dy\} \quad (1)$$

Euler-Lagrange equation can be obtained by (1):

$$\begin{cases} \mathbf{u} = \mathbf{f} - \lambda \Delta \left(\nabla \left(\frac{\nabla \mathbf{u}}{|\nabla \mathbf{u}|} \right) \right), & \text{in } \partial\Omega \\ \frac{\partial \mathbf{u}}{\partial \mathbf{n}} = 0, \frac{\partial}{\partial \mathbf{n}} \left(\nabla \left(\frac{\nabla \mathbf{u}}{|\nabla \mathbf{u}|} \right) \right) = 0, & \text{on } \partial\Omega \end{cases} \quad (2)$$

Equation (2) is a fourth-order equations with computational complexity and exist convergence speed problem, $\sqrt{|\nabla \mathbf{u}|^2 + \varepsilon^2}$ is commonly used to approximate $|\nabla \mathbf{u}|$, where $\varepsilon \rightarrow 0$. However, in some cases, \mathbf{u} is very sensitive to the parameters ε , namely, if ε is too large, it will blur the edges of image; If ε is too small, we may get an error numerical solution. Therefore, we would not get image decomposition effectively.

A staircase effect is exist for those denoised images by using ROF model, resulting in the loss of the image information. Chan and Esedoglu [13] replaced the data item of ROF model with $\int_{\Omega} |\mathbf{u}-\mathbf{f}| dx dy$, this model effectively improved the loss of geometric features. Therefore, this paper introduces the improved data item into OSV model. Equation (1) can be rewritten as

$$\min_u \left\{ E(u) = \int_{\Omega} |\nabla u| dx dy + \frac{1}{\lambda} \int_{\Omega} |\nabla(\Delta^{-1}(f-u))| dx dy \right\} \quad (3)$$

In order to reduce the computational complexity and improve convergence rate, we propose Multiple Auxiliary Variable Method (MAVM) and introduce it into (3). More specifically shown in the following

$$\begin{aligned} w_1 &\approx \nabla u, \quad w_3 \approx \nabla w_2 \\ w_2 &\approx (\nabla^{-1})(u-f) \Rightarrow \Delta w_2 = u-f \\ \min_{u, w_1, w_2, w_3} &\left\{ \begin{aligned} &E(u, w_1, w_2, w_3) = \int_{\Omega} |w_1| dx dy + \frac{1}{\lambda} \int_{\Omega} |w_3| dx dy \\ &+ \frac{1}{2\theta_1} \int_{\Omega} (w_1 - \nabla u - b^{k+1})^2 dx dy \\ &+ \frac{1}{2\theta_2} \int_{\Omega} (u-f - \Delta w_2)^2 dx dy \\ &+ \frac{1}{2\theta_3} \int_{\Omega} (w_3 - \nabla w_2)^2 dx dy \end{aligned} \right\} \quad (4) \end{aligned}$$

where w_2 is a scalar, w_1, w_2, b are vectors.

$$b^{k+1} = b^k + \nabla u^k - w^k \quad (5)$$

The solution for (4) can be converted into the following functional problems, therefore, (4) can be rewritten as

$$\min_u \left\{ \begin{aligned} &E_1(u) = \frac{1}{2\theta_1} \int_{\Omega} (w_1 - \nabla u - b^{k+1})^2 dx dy \\ &+ \frac{1}{2\theta_2} \int_{\Omega} (u-f - \Delta w_2)^2 dx dy \end{aligned} \right\} \quad (6)$$

$$\min_{w_1} \left\{ \begin{aligned} &E_2(w_1) = \int_{\Omega} |w_1| dx dy \\ &+ \frac{1}{2\theta_1} \int_{\Omega} (w_1 - \nabla u - b^{k+1})^2 dx dy \end{aligned} \right\} \quad (7)$$

$$\min_{w_2} \left\{ \begin{aligned} &E_3(w_2) = \frac{1}{2\theta_2} \int_{\Omega} (u-f - \Delta w_2)^2 dx dy \\ &+ \frac{1}{2\theta_3} \int_{\Omega} (w_3 - \nabla w_2)^2 dx dy \end{aligned} \right\} \quad (8)$$

$$\min_{w_3} \left\{ E_4(w_3) = \frac{1}{\lambda} \int_{\Omega} |w_3| dx dy + \frac{1}{2\theta_3} \int_{\Omega} (w_3 - \nabla w_2)^2 dx dy \right\} \quad (9)$$

The corresponding solutions are obtained as follows

$$u^{k+1} = f + \Delta w_2^k + \frac{\theta_2}{\theta_1} (\Delta u^k + \nabla b^{k+1} - \nabla w_1^k) \quad (10)$$

$$w_1^{k+1} = \text{Max}(|\nabla u^{k+1} + b^{k+1}| - \theta_1, 0) \frac{\nabla u^{k+1} + b^{k+1}}{|\nabla u^{k+1} + b^{k+1}|} \quad (11)$$

$$\Delta(\Delta w_2) - \frac{\theta_2}{\theta_3} \Delta w_2 = \Delta u^k - \Delta f - \frac{\theta_2}{\theta_3} \nabla w_3^{k+1} \quad (12)$$

$$w_3^{k+1} = \text{Max}(|\nabla w_2^{k+1} - \frac{\theta_3}{\lambda}|, 0) \frac{\nabla w_2^{k+1}}{|\nabla w_2^{k+1}|} \quad (13)$$

Where (10) use an explicit iteration method, (12) use a semi-implicit iterative method, (11) and (13) uses a soft threshold formula to evaluate the analytical solution. The algorithm is described as follows:

- (1) Initialization
 $w_{11}^0 = w_{12}^0 = w_2^0 = w_{31}^0 = w_{32}^0 = b_1^0 = b_2^0 = 0 \quad u^0 = f$;
- (2) Iteration: replaced f with u^k , complete alternative iteration of (6), (10), (11), (12) and (13);
- (3) Iterative termination criteria : stop running if satisfied with $\max(|u^{k+1} - u^k|) \leq \varepsilon$.

B. Results of Image Decomposition

In order to show the structure layer and texture layer obviously, OSV decomposition model is used for palmprint image. Fig. 1 and Fig. 2 shows that the structure layer remains unchanged with the degree of blur (σ) becomes larger and larger, the texture layer which changes dramatically, namely, the information in the texture layer is unstable.

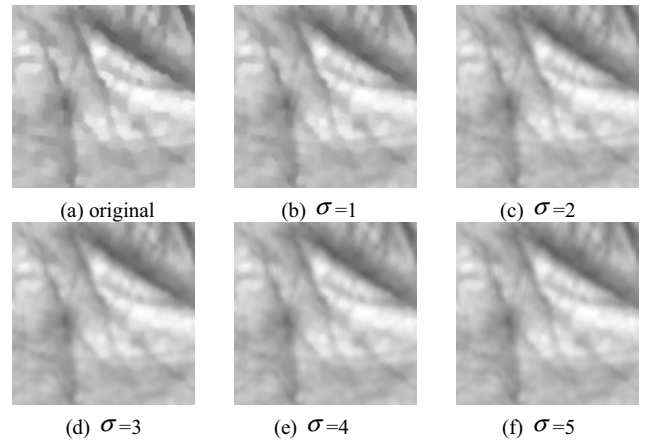


Figure 1. The structure layer with different degrees of blurring corresponding to Figure.2 obtained using the OSV decomposition model

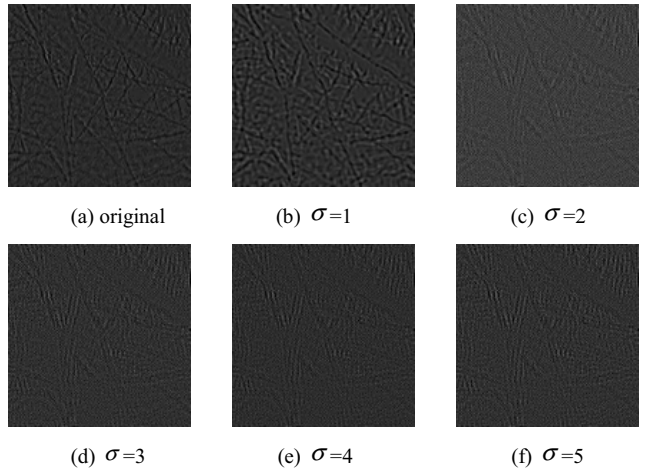


Figure 2. The texture layer with different degrees of blurring corresponding to Figure.2 obtained using the OSV decomposition model

Fig. 3 and Fig. 4 show the three-dimensional surface plots of structure layer and texture layer corresponding to Fig. 1 and Fig.2, which can be clearly observed the changes for structural layer and the texture layer when blurring. As

shown in Fig.3, structure layer contains main information of the image, Fig.4 shows that the feature is extremely unstable in the process of image blur. Hereby it can not be regarded as the stable image features.

According to the results of OSV decomposition, we know that the structure layer remains stable even if an image suffers from different degree of blurring. As a result, the structure layer of the image can be treated as a stable feature to recognize.

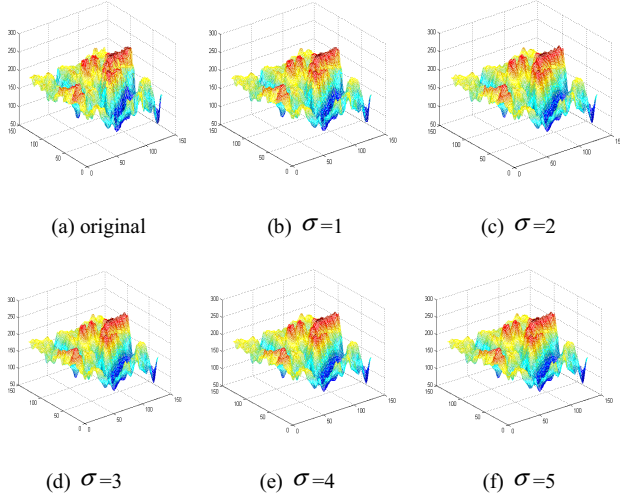


Figure 3. Surface plots of the structure layers corresponding to Figure 1

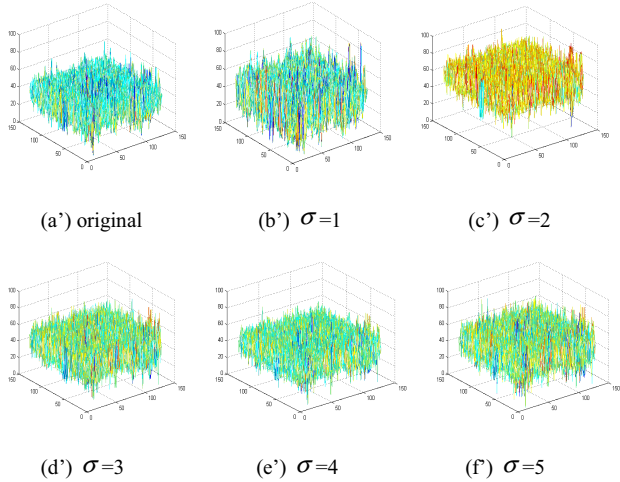


Figure 4. Surface plots of the texture layers corresponding to Figure 2

III. RECOGNITION ALGORITHM BASED ON SR-RISF

A. Image Down-sampling Based on Structure Ratio

We take the structure layer as the Relatively Invariant Structural Features (RISF) in the process of image blurring. Although the structure layer can keep relatively stability, the identification results are not good enough. Therefore, we use a non-overlapping sampling method based on Structure

Ratio (SR) for RISF to further improve the discrimination and effectiveness of feature, and obtaining the SR-RISF. This can be expressed as

$$M = \frac{\sum_{i=1}^m \sum_{j=1}^n I(i, j)}{m \times n} \quad (14)$$

$$S = \frac{\sum_{i=1}^m \sum_{j=1}^n (I(i, j) - M)^2}{m \times n} \quad (15)$$

$$SR = \frac{M}{S} \quad (16)$$

where I is a size of $m \times n$ non-overlapping sampling area of original palmprint image, i and j is corresponding pixel location of sampling area, M stands for grey average of sampling area, S is variance of sampling area, SR is structure ratio of sampling area.

We select the structure layer of blurring palmprint image ($\sigma = 3$) to test by using SR method, results can be seen from Fig. 5, it is difficult to visually distinguish the blurring image between A and B. (d)~(f) is the RISF obtained by OSV decomposition model, which could better distinguish the similar blurring image, (g)~(i) is the SR-RISF feature which needs further improve the discrimination of features for the palmprint image.

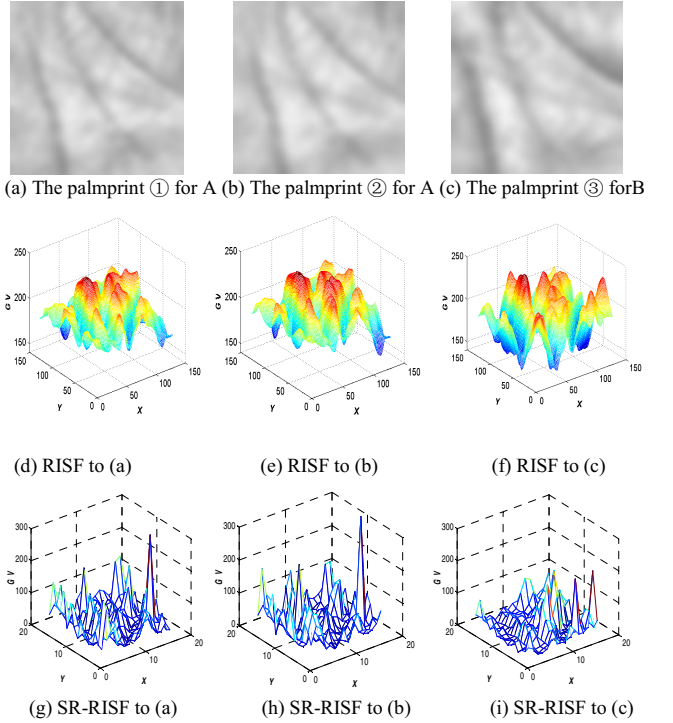


Figure 5. Blurred palmprint feature examples among the same people and the different people

B. Feature Matching for Blurring Palmprint Image

Structural Similarity Index Measurement (SSIM) [14] was introduced in this paper to measure the similarity between palmprint features. SSIM algorithm can describe

the structure features from three aspects which are the bright (L), contrast(C) and structure(S). Specifically shown as follows

$$L(x,y)=\frac{2\mu_x\mu_y+c1}{\mu_x^2+\mu_y^2+c1} \quad (17)$$

$$C(x,y)=\frac{2\sigma_x\sigma_y+c2}{\sigma_x^2+\sigma_y^2+c2} \quad (18)$$

$$S(x,y)=\frac{\sigma_{xy}+c3}{\sigma_x\sigma_y+c3} \quad (19)$$

Where x and y represent two structural features to be matched, μ_x and μ_y stand for to the average value of x and y , σ_x and σ_y stands for the variance of x and y , σ_{xy} is the covariance of x and y , small constants $c1, c2, c3$ are used to increase the stability of calculation results. We usually take $c1=(K_1 \times GVM)^2$, $c2=(K_2 \times GVM)^2$, $c3=c2/2$, $K_1 \ll 1$, $K_2 \ll 1$, GVM is the maximum grey value of palmprint image (typically take 255), SSIM value is determined by the values of L, C, S .

$$SSIM(x,y)=L(x,y) \times C(x,y) \times S(x,y) \quad (20)$$

Where SSIM value represents the similarity of two matched structural feature, the range is from 0 to 1. Therefore, we should set a threshold value $thres$ so that two palmprint image can be classified.

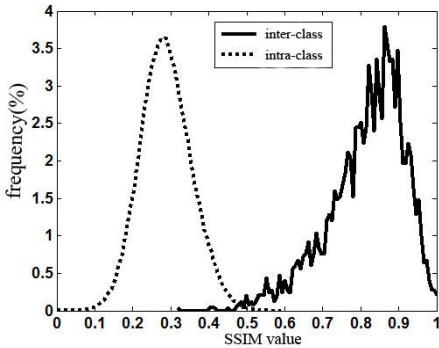


Figure 6. Curves of inter-class and intra-class

As can be seen from Fig.6, the value of inner-class curve of SSIM concentrates on the near side of the 1, the closer to 1, the higher similar of two blurred palmprint image, and the value of intra-class curve of SSIM concentrated on the near side of the 0, the closer to 0, the bigger difference between two blurred palmprint image. Therefore, an appropriate threshold of $thres$ (we can obtained the size of threshold by equal error rate curve [15], $thres = 0.4251$) can separate the palm more accurately and effectively.

IV. EXPERIMENTS AND RESULTS

The proposed method was implemented using MATLAB 2010a on a desktop PC with a modest CPU (2.9GHZ), and 4GB of random access memory. In order to reflect the relationship between FAR and FRR, a receiver operating characteristic (ROC) curve is constructed, which can

conveniently compared with different algorithms. We carried out 3 experiments on PolyU palmprint database and Blurred-PolyU palmprint database in order to verify the effectiveness of the proposed method.

A. Experiment 1

It is difficult to describe the characteristics if we directly use the structure layer as the characteristics to recognize, therefore, the size of the sampling area has a great influence on the final recognition results when we extract the feature of blurred palmprint image, and the optimal partitioning method are usually determined by experiment. Therefore, blocks of different size (4×4 , 8×8 , 16×16 , 32×32) are tested in the Blurred-PolyU palmprint database to choose the optimal regional block. Fig. 7 shows the ROC curve of different size sampling area for SR-RISF algorithm and RISF algorithm.

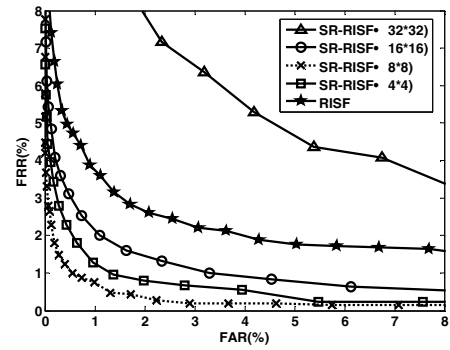


Figure 7. ROC curves obtained using different block size

Table I gives the corresponding equal error rate (EER), feature extraction time (FET), feature matching time (FMT) and recognition time (RT), RT is the time for an identity, which is defined as

$$RT=FET+FMT \times N_s \quad (21)$$

Where N_s is the number of template among training set in the palmprint system (usually take one image from one person as the training template), all the palms in palmprint database are captured from 386 different people, therefore, the value of N_s is 386.

TABLE I. EER, FET, FMT AND RT FOR RISF AND SR-RISF

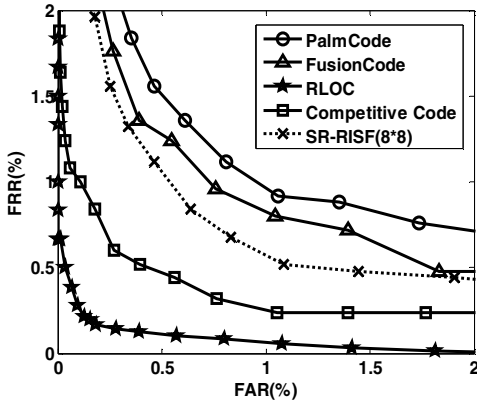
Algorithm	EER(%)	FET(ms)	FMT(ms)	RT(ms)
RISF	2.4676	12.71	4.87	1892.53
SR-RISF (4×4)	1.1406	39.75	2.48	985.45
SR-RISF (8×8)	0.8340	26.37	2.31	918.03
SR-RISF (16×16)	1.6118	21.09	2.21	874.15
SR-RIS (32×32)	4.8073	19.22	2.09	825.96

As can be seen from Fig. 7, the EERs obtained using the idea of block with size of 4×4 , 8×8 , 16×16 are lower than that of only using RISF algorithm, where the EER obtained

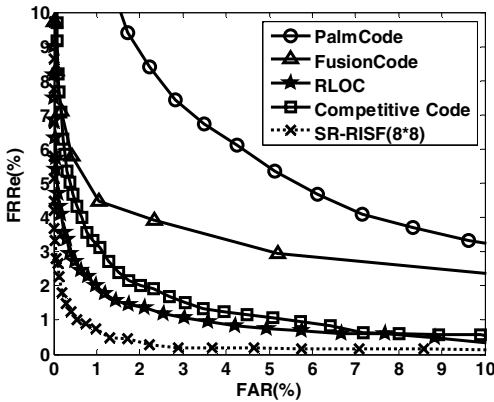
using 8×8 is the lowest, and EER value of 32×32 is higher than obtained using RISF algorithm. By considering the results in table, we can get a conclusion that the recognition time of RISF algorithm is the longest, but the bigger of block is, the smaller of recognition time it is. Hence, SR-RISF can obtain more discriminative features and reduce the recognition time if we choose the reasonable sampling size. In addition, the EER of SR-RISF (8×8) is the lowest and the RT is 918.03 ms, therefore, the optimal size of sampling size in this paper is 8×8 .

B. Experiment 2

In order to verify the proposed SR-RISF method could extract the stable feature, we performed experiments using the PolyU and blurred-PolyU palmprint databases, and making comparison with some high-performance methods on PolyU palmprint database (Palm Code [16], Fusion Code [7], Competitive Code [8], RLOC [17]).



(a) ROC curves on the PolyU database



(b) ROC curves on the Blurred-PolyU database

Figure 8. ROC curves between SR-RISF and traditional high-performance algorithms on the different palmprint databases

Fig. 8(a) is the ROC curves for SR-RISF method and classical algorithm on the PolyU palmprint databases, where the EER of SR-RISF is lower than those obtained using Palm

Code and Fusion Code methods, but higher than Competitive Code and RLOC. Fig. 8(b) shows that the EER of SR-RISF is lower than those obtained using other classical algorithm on blurred-PolyU palmprint databases.

A conclusion can be obtained when compared Fig.8 (a) with Fig.8 (b) that the EER of SR-RISF method is relatively stable both in PolyU and blurred-PolyU palmprint databases. Table II lists the EER values corresponding to Fig. 8.

TABLE II. EER VALUES CORRESPONDING TO FIG.8

Algorithm	EER (%)	
	PolyU database	Blurred-PolyU database
PalmCode	0.9706	5.2653
FusionCode	0.8876	3.5215
Competitive Code	0.4792	2.0812
RLOC	0.1657	1.5250
SR-RISF (8×8)	0.7489	0.8340

Recognition methods based on coding (Palm Code, Fusion Code, Competitive Code, RLOC) can better describe the palmprint texture information, and gain a higher recognition accuracy. However it is difficult to represent the texture information for blurred images due to the loss of texture information. Therefore, the identification results of coding method are generally poor on the Blurred-PolyU palmprint database. However, the proposed method (SR-RISF) can extract the relatively stable features of blurred images, as a result the identification accuracy and robustness of the SR-RISF is higher than those of traditional high-performance algorithms.

C. Experiment 3

With the fast development of non-contact palmprint identification system, more and more scholars are interested in it, some classical algorithms of blurred palmprint recognition are proposed, such as 2DPCA [12], LBP [18], LST [3], DCT-PLC [1]. Fig. 9 shows the ROC curves of SR-RISF and some classical algorithms for blurred palmprint recognition on the Blurred-PolyU palmprint database. Table III is EER values corresponding to Fig. 9.

Fig. 9 and table III imply that the EER value of SR-RISF algorithm is the lowest, which shows the effectiveness of the proposed method. For the other methods, 2DPCA is the algorithm based on subspace, which can reflect the main information of the image, however, this method ignores the spatial structure information, and the identification accuracy is not high. LBP is a kind of algorithm by encoding the spatial texture information, although it can represent the spatial structure information of the image, but it really depends on texture information, and hence its accuracy is not high for blurred palmprint recognition. LST and DCT-PLC can extract the low frequency coefficients as the stable features of blurred images, which can reflect the main information of image, but both lack the description ability for the image spatial structure.

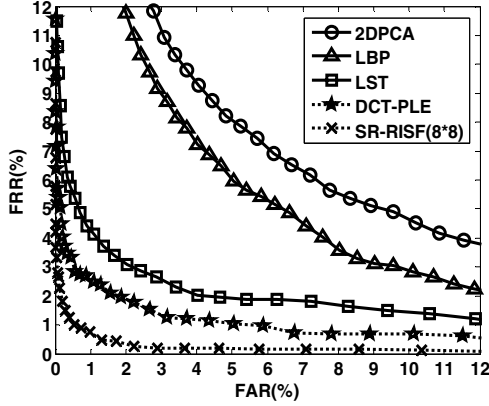


Figure 9. ROC curves between SR-RISF and classical blurred palmprint recognition methods on the Blurred-PolyU palmprint database

TABLE III. EER VALUES CORRESPONDING TO FIG.9

Algorithm	EER (%)
2DPCA	6.7790
LBP	5.5750
LST	2.7208
DCT-PLE	1.9249
SR-RISF (8 × 8)	0.8340

As a consequence, the distinguish ability is not high if we only use the low frequency coefficients as features to recognize the blurred palmprint image. On contrast, the SR-RISF algorithm proposed in this paper not only better describe the image spatial structure but also efficiently obtain the main information of images.

V. CONCLUSIONS

The proposed method in this paper could obtain higher identification accuracy and strong stability when compared with the traditional classical recognition methods, and meanwhile the robustness is higher for noise, blurriness and illumination. However, the method proposed in this paper need to determine the size of the sampling area before we used the non-overlapping sampling method, because the size of block has a great influence on the final recognition results. Therefore, based on the result obtained in this paper, the main do researches on how to obtain the optimal block automatically may be our direction for next step.

ACKNOWLEDGMENT

This work was financially supported by the National Natural Science Foundation of China (No.61170106) and Shandong Province Higher Educational Science and Technology Program (J14LN39).

REFERENCES

- [1] Sen Lin, Weiqi Yuan, Wei Wu, Ting Fang, Blurred palmprint recognition based on DCT and block energy of principal line [J]. Journal of Optoelectronics-Laser, 2012, 23(11):2200-2206.
- [2] Danfeng Hong, Zhenkuan Pan, Xin Wu, Improved Differential Box Counting with Multi-scale and Multi-direction: A New Palmprint Recognition Method [J]. Optik- International Journal of Light Electron Optics, 2014, 125(15), 4154-4160.
- [3] Sen Lin, Weiqi Yuan, Blurred palmprint recognition under defocus status [J]. Optics and Precision Engineering, 2013:21(3):734-741.
- [4] Danfeng Hong, Wanquan Liu, Jian Su, Zhenkuan Pan, Xin Wu, Robust Blurred Palmprint Recognition Based on the Fast Vese-Osher Model [J]. Communications in Computer and Information Science, 2014, 462: 228-238.
- [5] David Zhang, Waikin Kong, Jane You, Michael Wong, Online Palmprint Identification[J]. IEEE Transactions on Pattern Analysis and Machine Intelligence, 2003, 25(9):1041-1050.
- [6] Wei Jia, De-Shuang Huang, David Zhang, Palmprint Verification Based on Robust Line Orientation Code[J]. Pattern Recognition, 2008, 41(5): 1521-1530.
- [7] Choras M, Kozik R. Contactless palmprint and knuckle biometrics for mobile devices [J]. Pattern Analysis and Application, 2012,15(1):73-85.
- [8] Kanhangad V, Kumar A, David Zhang, A unified framework for contactless hand verification [J].IEEE Transactions on Information Forensics and Security, 2011,6(3):1014-1027.
- [9] Weiqi Yuan, Suyue Feng, Simulation system of improved non-contact on-line palmprint recognition [J]. Acta Optica Sinica, 2011,31(7):0712003.
- [10] Kang B J, Park K R. Real-time image restoration for iris recognition systems [J]. IEEE Transactions on Systems, Man, and Cybernetics, Part B: Cybernetics, 2007,37(6):1555-1566.
- [11] Guodong Wang, Jie Xu, Zhenkuan Pan, Cunliang Liu, Jinbao Yang, Blind image restoration based on normalized hyper laplacian prior term [J]. Optics and Precision Engineering, 2013, 21(5):1341-1347.
- [12] Fang Liu, Haifeng Sang, Defocused palmprint recognition using 2DPCA[C]. Proceedings of International Conference on Artificial Intelligence and Computational Intelligence, Shanghai, China, 2009:611-615.
- [13] Chan T, Esedoglu S, Aspects of Total Variation Regularized L1 Function Approximation. SIAM J. Appl. Math, 2005, 65(5): 1817 — 1837.
- [14] Shengnan Ye, Kaina Su, Chuangbai Xiao, Juan Duan, Image Quality Assessment Based on Structural Information Extraction[J]. Acta Electronica Sinica, 2008,36(5) : 856-861.
- [15] Danfeng Hong, Wanquan Liu, Jian Su, Zhenkuan Pan, Guodong Wang, A Novel Hierarchical Approach for Multispectral Palmprint Recognition [J]. Neurocomputing, 2015, 151:511-521.
- [16] Waikin Kong, David Zhang, Kamel M, Palmprint Identification Using Feature-level Fusion[J]. Pattern Recognition, 2006, 39(3): 478-487.
- [17] Feng Yue, Wangmeng Zuo, David Zhang, Kuanquan Wang, Orientation Selection using modified FCM for Competitive Coding-Based Palmprint Recognition[J]. Pattern Recognition, 2009, 42(11): 2841-2849.
- [18] Zhenhua Guo, Lei Zhang, David Zhang, A Completed Modeling of Local Binary Pattern Operator for Texture Classification. IEEE Transactions on Image Processing, 2010, 19(6): 1657-1663.